Waves in a hot uniaxial plasma excited by a current source

N. Singh* and R. W. Gould†

California Institute of Technology, Pasadena, California 91109

(Received 26 April 1971; final maniscript received 28 August 1972)

The fields excited by a short dipole antenna in a hot uniaxially anisotropic plasma ($B_0 \to \infty$) have been studied. When $\omega < \omega_p$, the dipole effectively excites two propagating waves, a slow wave and a fast wave, inside a cone of half-cone angle $\sin^{-1}(\omega/\omega_p)$. Inside the cone a characteristic interference structure in the angular distribution of the fields is noted. Outside the cone fields fall off exponentially. The appearance of the cone and the characteristic interference structure in the field is useful from the viewpoint of laboratory diagnostics.

I. INTRODUCTION

The excitation of the anisotropic plasma by a localized current source has been considered by several investigators.[1–6] They have investigated the radiation from simple current sources in a cold magnetoplasma from the point of view of impedance and far fields. Progress in the study of sources in magnetoplasma has been handicapped by the inherent difficulties encountered in modeling the plasma medium, and the inhomogeneous sheath region around the source. In the cold plasma approximation the medium is described by the usual Appleton–Hartree dielectric tensor, i.e.,

$$K = \epsilon_0 \begin{bmatrix} K_\perp & iK_H & 0 \\ -iK_H & K_\perp & 0 \\ 0 & 0 & K_{||} \end{bmatrix}, \tag{1a}$$

where

$$K_\perp = 1 - [\omega_p^2/(\omega^2 - \omega_c^2)],$$

$$K_H = [\omega_c \omega_p^2/\omega(\omega^2 - \omega_c^2)], \tag{1b}$$

and

$$K_{||} = 1 - (\omega_p^2/\omega^2).$$

Here, ω, ω_c, and ω_p are the source, the electron cyclotron, and the plasma frequencies, respectively. For some values of ω, ω_c, and ω_p this approximation does yield physically acceptable results, while for other values for which the indices of refraction have poles, it fails to give physically reasonable results. It occurs when $K_\perp$ and $K_{||}$ are of the opposite signs. In such cases, Kuehl[3] has shown that the fields of an infinitesimal dipole are singular on a conical surface and the nature of the singularity is such that the Poynting vector is also singular on the conical surface, yielding infinite power radiation from the source. The opening θ_0 of the conical surface depends upon ω, ω_c, and ω_p.

When the refractive index has a pole, the plasma medium is resonant[7] along some directions, where the wave vector ($\mathbf{k}$) is infinite and the phase velocity V_p vanishes. The cold plasma approximation is valid only when the phase velocity is much greater than the electron thermal velocity $V_0 = (kT_e/m_e)^{1/2}$, where T_e and m_e are the electron temperature and mass, respectively, and K is the Boltzmann constant. In the event of vanishing phase velocity, electron thermal motions are important.

In this paper it is shown that the addition of electron temperature to the theory removes the singularity from the fields. Here, both the near and the far fields are considered. The impedance calculation has been reported elsewhere.[8]

For a general anisotropic plasma, the problem is very difficult. Therefore, we have considered a uniaxial plasma ($B_0 \to \infty$). In the limit of large B_0, the perpendicular thermal motion of the electrons is not important. The sheath is still ignored. For a cold uniaxially anisotropic plasma $K_\perp = 1$, and $K_{||} = 1 - \omega_p^2/\omega^2$; therefore, $K_\perp/K_{||} < 0$ only when $\omega < \omega_p$. Then, the half-cone angle $\theta_0 = \sin^{-1}(\omega/\omega_p)$. In this paper the case $\omega < \omega_p$ has been considered.

It is important to mention that this work was motivated by the experiments of Fisher and Gould[9–11] in which they discovered a characteristic interference structure in the angular distribution of the fields excited by a probe in a magnetoplasma. This theory verifies the experimental results.

II. BASIC EQUATIONS

We consider an infinite and homogeneous plasma biased with an infinite magnetic field $\mathbf{B}_0$ in the z direction of the rectangular coordinate system. The filamentary dipole of length ($2l$) is assumed to be oriented along $\mathbf{B}_0$ (see Fig. 1). The current density on the antenna is given by

$$\mathbf{J}_s(\rho, z) = [\delta(\rho)/2\pi\rho] J_s(z)\, \mathbf{e}_z, \tag{2}$$

where $\mathbf{e}_z$ is a unit vector along the z direction and $J_s(z)$ gives the current distribution.

In order to treat the problem, Maxwell equations are solved with steady-state dependence $\exp(-i\omega t)$ and the plasma permittivity tensor

$$K = \epsilon_0 \begin{bmatrix} 1 & 0 & 0 \\ 0 & 1 & 0 \\ 0 & 0 & K_{||} \end{bmatrix}, \tag{3}$$

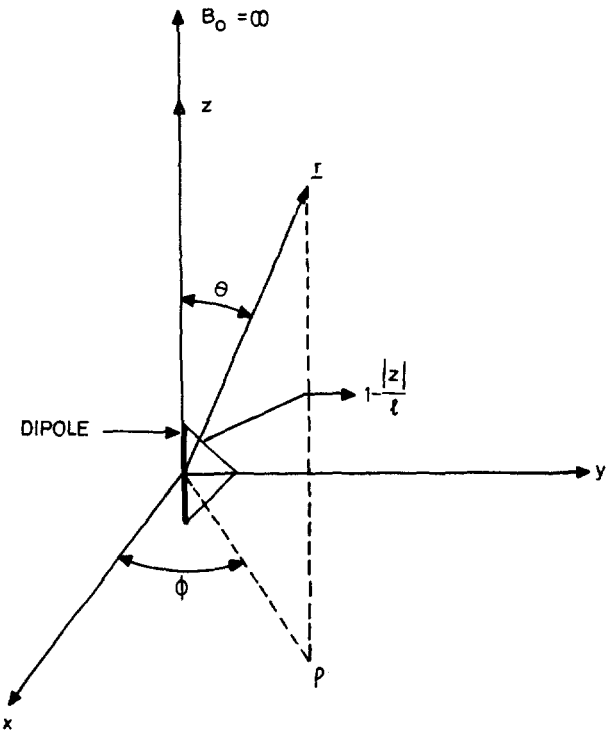

FIG. 1. Geometry of the problem. The triangular current distribution on the dipole is shown.

where $K_{||}$ is given by

$$K_{||}=1-(\omega_p^2/k_z^2V_0^2)Z'[(\omega+i\nu)/k_zV_0], \qquad (4)$$

and where Z' is the derivative of the plasma distribution function Z,[12] ν is the collision frequency, k_z is the wavenumber in the z direction, and V_0 is the electron thermal velocity defined by $V_0=(2KT_e/m_e)^{1/2}$, K is the Boltzmann constant, and T_e and m_e are the electron temperature and mass, respectively.

Since the B_0 is infinite, the plasma current flows only in the z direction. The dipole current is also in the z direction. Therefore, the dipole excites only three field components: E_z, E_ρ, and H_φ. The Fourier transform of the field $E_z(\rho, z)$ given by

$$\hat{E}_z(\rho, k_z)=\int_{-\infty}^{\infty} E_z(\rho, z)\exp(-ik_zz)\,dz, \qquad (5)$$

can easily be shown to satisfy the following differential equation:

$$\left(\frac{\partial^2}{\partial\rho^2}+\rho^{-1}\frac{\partial}{\partial\rho}+\alpha^2\right)\hat{E}_z(\rho, k_z) = -i\omega\mu_0\left(1-\frac{k_z^2}{k_0^2}\right)\frac{\delta(\rho)}{2\pi\rho}\hat{J}_z(k_z), \qquad (6)$$

where

$$\alpha=[K_{||}(k_0^2-k_z^2)]^{1/2}, \qquad k_0=\omega(\mu_0\epsilon_0)^{1/2}, \qquad (7)$$

and $\hat{J}_z(k_z)$ is the Fourier transform of $J_z(z)$. The other field components are found in terms of $\hat{E}_z(\rho, k_z)$:

$$\hat{E}_\rho(\rho, k_z)=\frac{ik_z}{(k_0^2-k_z^2)}\frac{\partial}{\partial\rho}\hat{E}_z(\rho, k_z), \qquad (8)$$

$$\hat{H}_\varphi(\rho, k_z)=\frac{i\omega\epsilon_0}{(k_0^2-k_z^2)}\frac{\partial}{\partial\rho}\hat{E}_z(\rho, k_z). \qquad (9)$$

Now, Eq. (6) can easily be solved to give

$$\hat{E}_z(\rho, k_z)=-\tfrac{1}{4}(\omega\mu_0)(1-k_z^2/k_0^2)\hat{J}_z(k_z)H_0^{(2)}(\rho\alpha). \qquad (10)$$

Since in Eq. (10) the Hankel function of the second kind is allowed, the sign of α in Eq. (7) must be chosen so that $\mathrm{Im}(\alpha)<0$.

The field as a function of space coordinates is found by the Fourier inversion of Eq. (10), i.e.,

$$E_z(\rho, z)=-\frac{\omega\mu_0}{8\pi}\int_{-\infty}^{\infty}dk_z\left(1-\frac{k_z^2}{k_0^2}\right)\hat{J}_z(k_z)H_0^{(2)}(\rho\alpha) \times\exp(ik_zz). \qquad (11)$$

The evaluation of the integral in Eq. (11) is the subject of the next two sections.

III. FAR FIELDS

In order to find the far fields, the integral in Eq. (11) is evaluated by the saddle-point method. It is convenient to introduce the spherical coordinate system through $\rho=r\sin\theta$ and $z=r\cos\theta$, $r>0$, $0<\theta<\pi/2$. For large r, $(\rho\alpha)$ can be made large provided θ and α are not zero. Then, the Hankel function $H_0^{(2)}(\rho\alpha)$ can be replaced by its asymptotic representation, i.e.,

$$H_0^{(2)}(\alpha r\sin\theta)\simeq(2/\pi r\alpha\sin\theta)^{1/2} \times\exp[-i(\alpha r\sin\theta-\pi/4)]; \qquad (12)$$

α has zero only at $k_z=\pm k_0$. But, the integrand in Eq. (11) vanishes at $k_z=\pm k_0$. Therefore, the contribution to the integral in Eq. (11) from the vicinity of $k_z=\pm k_0$ is negligible and E_z can be approximated by

$$E_z(r, \theta)\simeq-\frac{\omega\mu_0}{4\pi}(2\pi r\sin\theta)^{-1/2}\exp(i\tfrac{1}{4}\pi) \times\int_{-\infty}^{\infty}F(k_z)\exp[irQ(k_z, \theta)]\,dk_z, \qquad (13)$$

where

$$F(k_z)=\frac{\hat{J}_z(k_z)[1-(k_z^2/k_0^2)]}{\alpha^{1/2}} \qquad (14)$$

and

$$Q(k_z, \theta)=-\alpha\sin\theta+k_z\cos\theta.$$

The asymptotic expression for the integral in Eq. (13) can be obtained by the saddle-point method.[13] The main contribution to the integral comes from the small regions near the saddle points k_{zi} given by

$$\frac{dQ_r(k_z,\theta)}{dk_z}=0$$

or

$$\frac{d}{dk_z}\alpha_r|_{k_z=k_{zi}}=\cot\theta, \qquad 0<\theta<\pi/2, \qquad (15)$$

where Q_r and α_r are the real parts of Q and α, respectively. Equation (15) can be solved numerically. A plot of saddle points k_{zi} against θ for $\omega_p/\omega=\sqrt{2}$ and $V_0/c=0.01$ is given in Fig. 2. It can be shown that for $k_zV_0/\omega>0.3$, Imα becomes quite large and thus the saddle points $k_{zi}>0.3\omega/V_0$ will not make significant contribution to the far field. Also, Imα is found to be quite large for $0<(k_zV_0/\omega)<0.01$. Then, the saddle points lying only in the range $0.01<(k_{zi}V_0/\omega)<0.3$ make a significant contribution to the far fields. These saddle points lying in the range $0.01<(k_{zi}V_0/\omega)<0.3$ give rise to two propagating waves, a slow wave and a fast wave, along a direction θ. These waves propagate only within a cone of half-cone angle θ_0. The angle θ_0 is slightly less than $\sin^{-1}(\omega/\omega_p)$. The fast and the slow waves correspond to the saddle points k_{z1} and k_{z2}, respectively. It should be noted that the slow wave does not propagate near the z axis; it is heavily damped. The asymptotic expression for the two waves for $\theta<\theta_0$ can easily be obtained by the saddle-point method:

$$E_z(r,\theta)\simeq-\frac{\omega\mu_0}{4\pi r}\frac{F(k_{z1})}{[\sin\theta\,|\,Q_r''(k_{z1},\theta)\,|]^{1/2}}$$

$$\times\exp[irQ_r(k_{z1},\theta)+\frac{i\pi}{2}+\mathrm{Im}\alpha(k_{z1})r\sin\theta]$$

$$-\frac{\omega\mu_0}{4\pi r}\frac{F(k_{z2})}{[\sin\theta\,|\,Q_r''(k_{z2},\theta)\,|]^{1/2}}$$

$$\times\exp[irQ_r(k_{z2},\theta)+\mathrm{Im}\alpha(k_{z2})r\sin\theta], \qquad \theta<\theta_0, \quad (16)$$

where the prime denotes differentiation with respect to k_z. From the foregoing expression for $E_z(r,\theta)$ we see that the fields fall as $1/r$. The net field inside the cone will be the interference of the two waves. The structure of the interference pattern will depend upon the relative amplitude of the two waves.

As one approaches the conical surface $\theta=\theta_0$, the two saddle points coalesce and then $Q_r''=0$. The saddle points become of second order. Then, the expression for $E_z(r,\theta)$ given by Eq. (16) must be improved. In order to obtain a valid asymptotic representation of the field near the cone, the term $(k_z-k_{zi})^3$ in the Taylor expansion of $Q_r(k_z,\theta)$ near $k_z=k_{zi}$ must be included. We

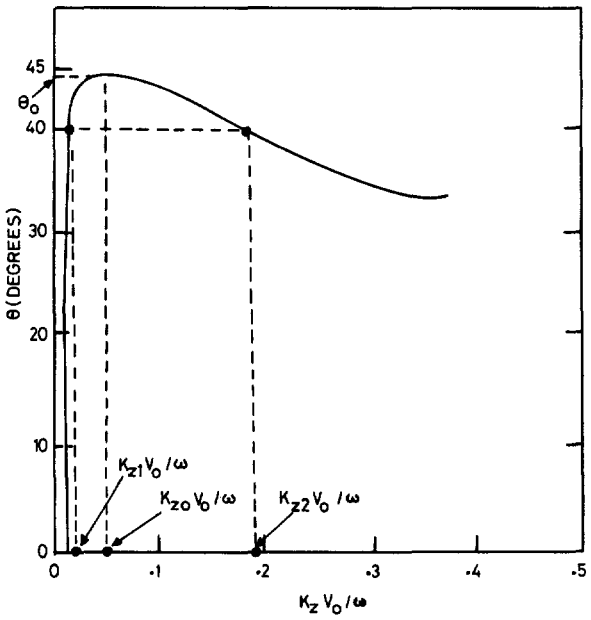

FIG. 2. The saddle-point plot for $c/V_0=100$ and $\omega_p/\omega=2^{1/2}$.

therefore expand $Q_r(k_z,\theta)$ about $k_z=k_{z0}$, and $\theta=\theta_0$ in a double Taylor series and keep terms up to the third order in (k_z-k_{zi}) and first order in $(\theta-\theta_0)$. Thus, we have

$$Q_r(k_z,\theta)\simeq A+B\tilde{\theta}-(\sin\theta_0)^{-1}\tau\tilde{\theta}-(3!)^{-1}\alpha_r'''(k_{z0})\sin\theta_0\tau^3, \qquad (17)$$

where $A=Q_r(k_{z0},\theta_0)$, $B=(d/d\theta)Q_r(k_{z0},\theta)\,|_{\theta=\theta_0}$, and $\tilde{\theta}=(\theta-\theta_0)$ and $\tau=(k_z-k_{z0})$. Then, combining Eqs. (13) and (17) we obtain

$$E_z(r,\theta)\simeq-[\omega\mu_0F(k_{z0})/(r\sin\theta_0)^{5/6}]$$
$$\times[(2)^{1/2}\alpha_r'''(k_{z0})]^{-1/3}[\mathrm{Ai}(X)/(\pi)^{1/2}]$$
$$\times\exp[ir(A+B\tilde{\theta})+i\pi/4+r\sin\theta_0\,\mathrm{Im}\alpha(k_{z0})] \qquad \theta\simeq\theta_0, \qquad (18)$$

where Ai(X) is the Airy function and X is given by

$$X=\tilde{\theta}[2r^2/\alpha_r'''(k_{z0})\sin^4\theta_0]^{1/3}. \qquad (19)$$

The Airy function Ai(X) is oscillatory for $X<0$ and exponentially decaying for $X>0$. Thus, the field is oscillatory with decreasing amplitude inside the cone $(\theta<\theta_0)$ and exponentially decreasing outside the cone $(\theta>\theta_0)$.

From Eq. (19) the structure of the pattern near the cone surface can be predicted. The spacing $\Delta\theta$ between two adjacent maxima or minima of the field pattern near the cone will be given by

$$\Delta\theta=[\alpha_r'''(k_{z0})\sin^4\theta_0/2r^2]^{1/3}\Delta X, \qquad (20)$$

where ΔX is the spacing between two adjacent maxima or minima of $|\,\mathrm{Ai}(X)\,|$. It is clear that $\Delta\theta=r^{-2/3}$.

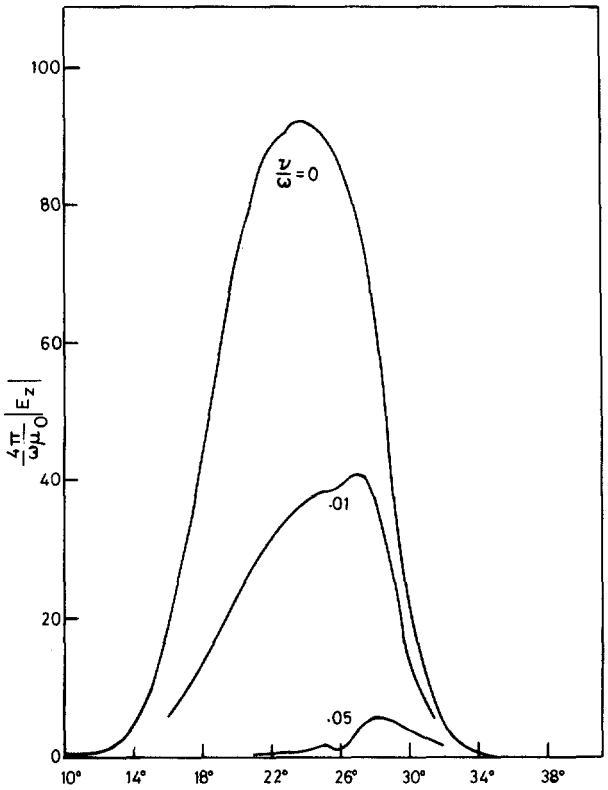

FIG. 3. Effects of collisional damping on the interference structure ($\omega_p/\omega=2$, $c/V_0=307$, $k_0r=1$, $k_0l=0.01$).

Since $k_{z0}\ll\omega/V_0$, in the vicinity of $k_z=k_{z0}$, $K_{||}$ can be approximated by

$$K_{||}=1-(\omega_p^2/\omega^2)[1+(3k_z^2V_0^2/2\omega^2)]. \quad (21)$$

Then we obtain

$$\alpha_r'''(k_{z0})\simeq\frac{18(\omega_p/\omega)^3}{[1-(\omega^2/\omega_p^2)]^{1/2}}\left(\frac{V_0}{\omega_p}\right)^2. \quad (22)$$

Combining Eqs. (20) and (22), we obtain for $\Delta\theta$ in degrees,

$$\Delta\theta^0\simeq 3.5\Delta X(\omega/\omega_p)^{1/3}[1-(\omega^2/\omega_p^2)]^{-1/6}(200V_0/\omega_p r)^{2/3}. \quad (23)$$

From Eq. (23) spacing between two adjacent maxima can be obtained. For example, for the first two maxima $\Delta X=2.2$. Since $(\omega/\omega_p)^{1/3}[1-(\omega^2/\omega_p^2)]^{-1/6}=\tan\theta_0$, Eq. (23) can be directly compared to Eq. (11) of Fisher and Gould.[11]

IV. NEAR FIELDS

The study of the near field of a probe or an antenna in a magnetoplasma is useful from the viewpoint of laboratory diagnostics. Measurements of the near field pattern can render information about the electron density and temperature. By numerical evaluation of the integral in Eq. (11) the effects of collisional and Landau damping, dipole length, electron thermal velocity, and distance from the source on the angular distribution of the near field pattern have been studied in this section. This study sheds some light on how to measure some of the plasma parameters in the laboratory. The results presented here are for a triangular current distribution on the dipole (see Fig. 1).

In the preceding section, it was found that the far field consists of two propagating waves, a slow wave and a fast wave, and these waves propagate only within a cone whose cone angle is slightly less than $\sin^{-1}(\omega/\omega_p)$. The numerical calculation of the near field demonstrates that two waves interfere within this cone and outside of this cone the field falls off rapidly.

A. Collision Damping

Figure 3 shows a field pattern of E_z. This figure has several interesting features. At a small collision frequency this pattern shows no interference. Only when the collision frequency is sufficiently large is the interference of the two waves in the angular distribution of the field pattern noted. In order that the two waves interfere and give several maxima and minima in the field patterns, the amplitudes of the two interfering waves should be comparable. Moreover, the slow wave is more susceptible to collision damping than the fast wave. In this case, for the value of parameters shown in Fig. 3, the dipole excites the slow wave much more than the fast wave. Collisional and Landau damping reduce the amplitude of the slow wave and thus make the amplitude of the two waves comparable at a certain distance from the source.

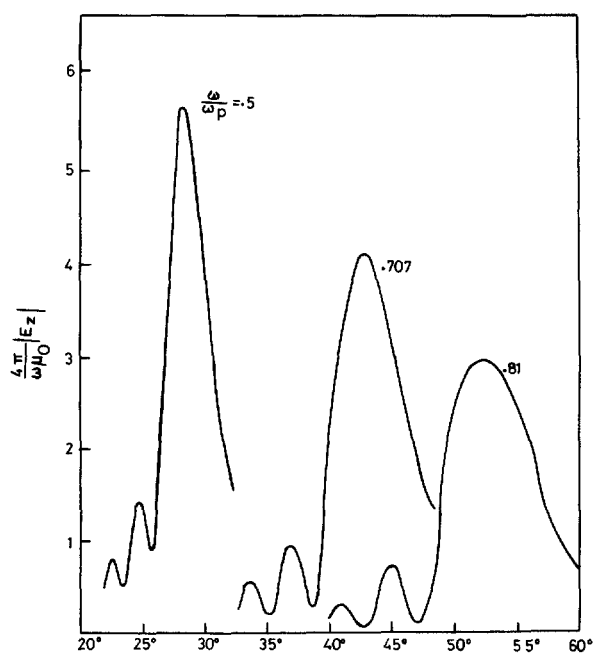

FIG. 4. Diagram showing well-defined maxima–minima in the angular distribution of the field ($k_0l=0.01$, $\nu/\omega=0.05$, $k_0r=1$, $c/V_0=307$).

Furthermore, it can be seen from Fig. 3 that by increasing the collision frequency the cone angle, where maximum in the field pattern occurs, moves closer to $\sin^{-1}(\omega/\omega_p)$. The appearance of the slow wave is a hot plasma effect. In the limit when the collision frequency tends to be large, temperature effects become less important and the results of the cold plasma theory with collisions can be recovered from this treatment.

The field patterns in Fig. 4 clearly demonstrate the interference phenomenon. These field patterns are for different values of ω/ω_p and $\nu/\omega=0.05$. Increasing ω/ω_p increases the cone angle, hence for a given value of r, the cone occurs at a larger radial distance ρ. Since $(\alpha\rho)$ is the argument of the Hankel function in the integral expression of Eq. (11), the slow waves are more damped. This gives interference patterns with well-defined maxima and minima. But, it is expected that when ω/ω_p is large enough for the slow waves to be completely damped out, the interference structure will disappear. The interference pattern with well-defined maxima and minima (at a certain distance r from the source) appears only for a certain range of values of ω/ω_p. The extent of the range depends on the distance r.

The experimental study of the field patterns by Fisher[14] compares qualitatively with these theoretical interference patterns. In this experiment the collision frequency is much smaller than the one used for obtaining the field patterns in Fig. 4. It is expected that the sheath around the probe in this experiment damps the slow wave which propagates inside the cone. Thus, it is possible for interference patterns with several maxima and minima to appear with a smaller collision frequency.

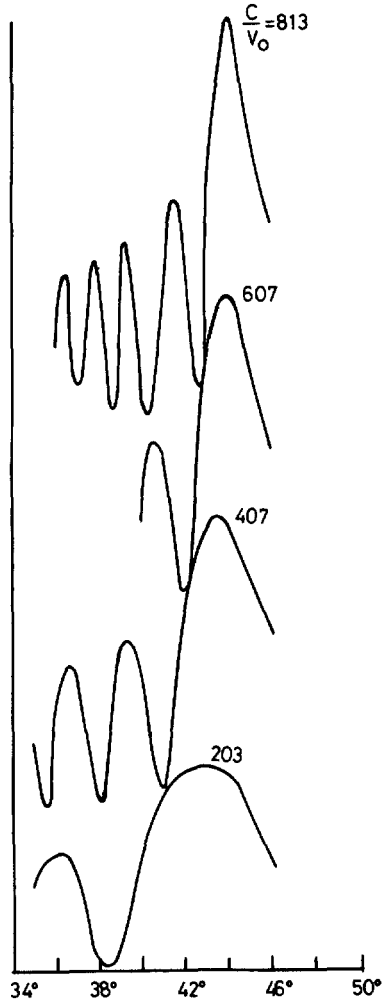

FIG. 6. Diagram showing increasing cone height and decreasing interference spacing $\Delta\theta$ with decreasing thermal speed $V_0(\omega_p/\omega=2^{1/2}, k_0r=1, k_0l=1)$.

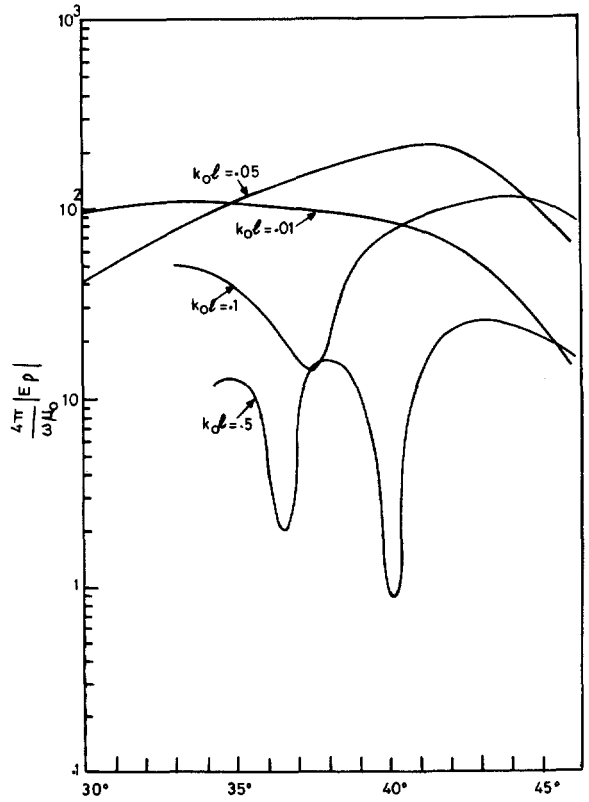

FIG. 5. Effect of dipole length on the interference structure $(c/V_0=307, \omega_p/\omega=2^{1/2}, k_0r=1)$.

B. Dipole Length

The length of a dipole in a magnetoplasma can play an important role in determining the field pattern. Angular distributions of the field for several dipole lengths are given in Fig. 5. For a very short dipole the field pattern shows no interference of the two waves. By increasing the length of the dipole, field patterns with several maxima and minima appear. This has the following simple explanation.

When the dipole is very short, it is a more effective radiator of the short wavelength waves, which are the slow waves, than of the fast ones. As the dipole becomes longer it radiates more fast waves and beyond a certain length it radiates less and less slow waves. Hence, when the dipole becomes long enough for the amplitudes of

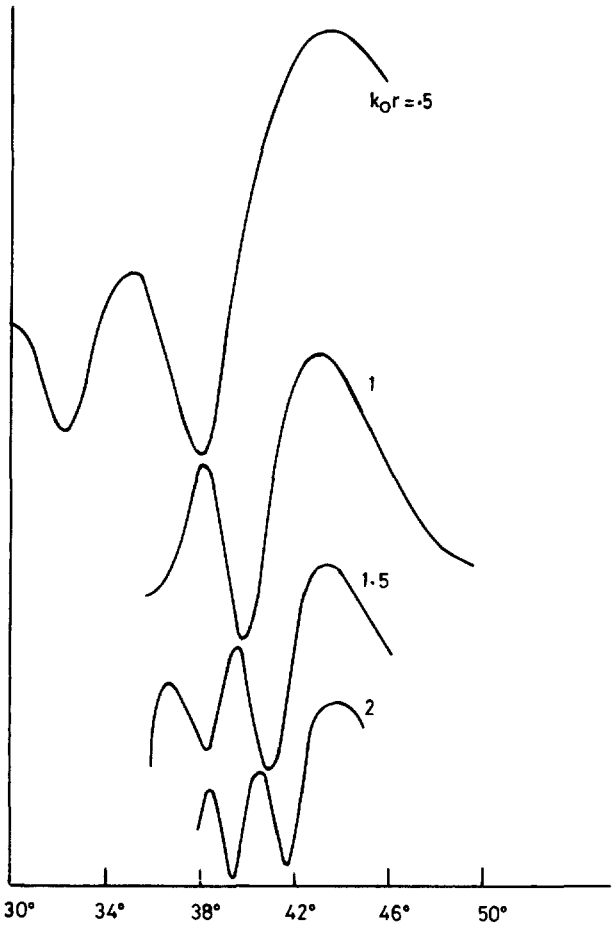

FIG. 7. Diagram showing decreasing cone height and decreasing spacing $\Delta\theta$ with increasing distance from the antenna ($k_0 l = 1$, $\omega_p/\omega = 2^{1/2}$, $c/V_0 = 307$).

the two waves to be comparable, they interfere to give several maxima and minima in the field pattern. When the dipole becomes too long, the fast wave becomes much larger than the slow wave, and then the interference structure disappears again.

C. Electron Thermal Velocity

The effect of the electron thermal velocity on the interference of the two waves and angular distribution of the field pattern is shown in Fig. 6. It can be seen from this figure that the height of the cone increases almost linearly with c/V_0.

Also the cone angle approaches $\sin^{-1}(\omega/\omega_p)$ as V_0 gets smaller. In the limit V_0 tends to zero; the fields become infinite on the conical surface of cone angle $\sin^{-1}(\omega/\omega_p)$. This is the result of the linear cold plasma theory. Hot plasma effects make the fields finite at this angle. The spacing $\Delta\theta$ between the two adjacent maxima and minima and the shift in the cone angle from $\sin^{-1}(\omega/\omega_p)$ goes as $(c/V_0)^{-2/3}$. The warmer the plasma, the greater the spacing $\Delta\theta$ and the shift in the cone angle. These results can be compared with the asymptotic representation of the fields near the cone in the preceding section.

D. Distance r from the Origin

Figure 7 gives field patterns for several values of the normalized distance ($k_0 r$). The height of the cone falls approximately as $r^{-2/3}$. The spacing $\Delta\theta$ between the two adjacent maxima or minima and the shift in the cone angle from $\sin^{-1}(\omega/\omega_p)$ behaves as $(k_0 r)^{-2/3}$. This has been verified experimentally by Fisher and Gould.[11] This behavior was also found from the asymptotic representation of the field near the cone in Sec. III. Combining the effects of thermal velocity and the distance, we obtain an expression for $\Delta\theta$ as given by Eq. (23).

E. Diagnostic Techniques

It was stated at the beginning of this section that the study of the near fields may be useful for diagnosing plasma in a magnetic field. Here, some experiments are mentioned for measuring the electron density and temperature. A measurement of the cone angle in the angular distribution of the field pattern of a probe in a magnetoplasma can give an estimate of the plasma density. The half-cone angle for a cold plasma is given by $\sin^{-1}(\omega/\omega_p)$. The electron temperature shifts this angle to a smaller value. A measurement of the spacing between the first two maxima can give an estimate of the electron temperature in terms of V_0. These experiments have been carried out by Fisher and Gould.

One must remember that the above considerations are valid only when the magnetostatic field B_0 is very large and the plasma density is low so that the cyclotron frequency $\omega_c \gg \omega_p$. The source frequency ω should be chosen so that $\omega < \omega_p$ for which the resonance cone in the field pattern appears. The appearance of the resonance cone in the field pattern is advantageous from the viewpoint of diagnostics in a small volume of laboratory plasma. In such a situation reflections from the walls do not appear to come back to the probe.

V. DISCUSSION

In this paper the fields excited by a short electric dipole antenna in a hot uniaxial plasma have been studied. The addition of the electron temperature to the theory modifies the cold plasma results substantially. The hot plasma effects give a finite field on the conical surface of half-cone angle $\sin^{-1}(\omega/\omega_p)$, where the fields are singular for a cold plasma. When $\omega < \omega_p$, the dipole effectively excites two propagating waves, a slow wave and a fast wave, inside the cone. Outside the cone, the fields are exponentially damped. The net field at any point inside the cone would be the result of the interference of the two waves. A characteristic interference structure in the angular distribution of the field is found. The interference spacing between the two adjacent maxima and minima near the cone surface

varies as $(V_0/\omega r)^{2/3}$. This is in agreement with the experimental results of Fisher and Gould.[9-11]

As suggested by Fisher and Gould,[11] the appearance of the cones and the interference structure in the angular distribution of the field can be used as a diagnostic tool for laboratory magnetoplasma. Because of the cones in the field pattern, the reflections from the walls of the plasma container do not appear to come to the source.

The results presented in this paper are for a dipole oriented along the magnetic field B_0. But, it is expected that the characteristic interference spacing near the resonance cone is not significantly affected by the dipole orientation. For an orientation other than parallel, a new mode with $k=\omega/c$ will be excited.[3] However, the amplitude of a wave in this mode near the cone surface will be small compared with the fast and the slow waves. Thus, only these later waves will interfere effectively with each other. Since the relative phase of these waves will be independent of the orientation of the dipole, the interference spacing $\Delta\theta$ will be approximately the same near the cone surface.

The length of the antenna plays an important role in exciting the waves. The characteristic interference structure will appear only over a range of the antenna length, that is, when the antenna is neither too short nor too long.

The theory given here ignores the sheath and assumes that $B_0=\infty$. There is, therefore, only a qualitative agreement between the theory and the experiment.[11] For a complete quantitative comparison between the theory and the experiment, one must deal with a finite magnetic field and include the sheath.

The sheath effectively introduces an attenuation factor and the slow waves are attenuated more than the fast waves. This has been demonstrated in a recent paper by Singh.[15]

The analysis with a finite magnetic field is difficult but some understanding of the effects of the finite magnetic field can be obtained by ignoring the perpendicular thermal motions of the electrons. Then, $K_\perp$ as given in Eq. (1) is not modified by the thermal velocity V_0. The resonance half-cone angle will be given by

$$\sin\theta_0=(\omega/\omega_p)[1+(\omega_p^2-\omega^2)/\omega_c^2], \qquad (24)$$

and Eq. (20) will be modified to

$$\Delta\theta=\Delta X[\alpha r'''(k_{z0})\sin^4\theta_0/K_\perp^{1/2}2r^2]^{1/3}. \qquad (25)$$

Still $\alpha_r'''(k_{z0})$ will be given by Eq. (22). After some algebraic manipulations, we find that for $\omega_c\gg\omega_p$

$$\Delta\theta_f/\Delta\theta_i=1+\tfrac{1}{3}(1.5\omega_p^2-2\omega^2)/\omega_c^2, \qquad (26)$$

where the subscripts f and i on $\Delta\theta$ are for the finite and infinite magnetic fields, respectively. We see that for small cone angles $\Delta\theta_f>\Delta\theta_i$ and on the other hand, for large cone angles $(\omega/\omega_p>\sqrt{3}/2)$ $\Delta\theta_f<\Delta\theta_i$. This could explain the observation of Fisher and Gould that the measured variation of $\Delta\theta$ with cone angle was, in general, somewhat flatter than $\tan^{1/3}\theta_0$.

ACKNOWLEDGMENTS

This research was supported in part by the Office of Naval Research under Contract No. 220(50) and in part by the Atomic Energy Commission under Contract AT(04-3)-767. The original manuscript was prepared under Atomic Energy Commission Contract AT(11-1)-2059.

* Present address: Department of Electrical Engineering, Indian Institute of Technology, Kanpur-16, India.
† Present address: The United States Atomic Energy Commission Washington, D.C. 20545.

[1] F. V. Bunkin, Zh. Eksp. Teor. Fiz. **32**, 338 (1957) [Sov. Phys. JETP **5**, 277 (1957)].
[2] H. Kogelnik, J. Res. Natl. Bur. Std. (U.S.) **64**, 515 (1960).
[3] H. H. Kuehl, Phys. Fluids **5**, 1095 (1962).
[4] H. Staras, Radio Sci. **1**, 1013 (1966).
[5] S. R. Seshadri, Proc. IEE **112**, 1856 (1965).
[6] K. G. Balmain, IEEE Trans. Antennas Propagation **AP-12**, 605 (1964).
[7] W. P. Allis, S. J. Buchsbaum, and A. Bers, *Waves in Anisotropic Plasmas* (MIT Press, Cambridge, Mass., 1963), Chap. 3.
[8] N. Singh, Ph.D. thesis, California Institute of Technology (1971); N. Singh and R. W. Gould, Bull. Am. Phys. Soc. **14**, 1004 (1969); N. Singh and R. W. Gould, Radio Sci. **5**, 1151 (1971).
[9] R. K. Fisher and R. W. Gould, Phys. Letters **31**, 235 (1970).
[10] R. K. Fisher and R. W. Gould, Phys. Rev. Letters **22**, 1093 (1969).
[11] R. K. Fisher and R. W. Gould, Phys. Fluids **14**, 857 (1971).
[12] B. D. Fried and S. D. Conte, *The Plasma Dispersion Function* (Academic, New York, 1961).
[13] E. T. Copson, *Asymptotic Expansions* (Cambridge University Press, Cambridge, 1965), Chap. 8.
[14] R. K. Fisher, Ph.D. thesis, California Institute of Technology (1970).
[15] N. Singh, Phys. Fluids (to be published).